AD

TECHNICAL REPORT ARCCB-TR-95013

TRANSLAMINAR FRACTURE TOUGHNESS TEST METHODS AND RESULTS FROM INTERLABORATORY TESTS OF CARBON/EPOXY LAMINATES

JOHN H. UNDERWOOD
MARK T. KORTSCHOT
W. RANDOLPH LLOYD
HARVEY L. EIDINOFF
DALE A. WILSON
NOEL ASHBAUGH

FEBRUARY 1995

US ARMY ARMAMENT RESEARCH,
DEVELOPMENT AND ENGINEERING CENTER
CLOSE COMBAT ARMAMENTS CENTER
BENÉT LABORATORIES
WATERVLIET, N.Y. 12189-4050

DISCLAIMER

The findings in this report are not to be construed as an official Department of the Army position unless so designated by other authorized documents.

The use of trade name(s) and/or manufacturer(s) does not constitute an official indorsement or approval.

DESTRUCTION NOTICE

For classified documents, follow the procedures in DoD 5200.22-M, Industrial Security Manual, Section II-19 or DoD 5200.1-R, Information Security Program Regulation, Chapter IX.

For unclassified, limited documents, destroy by any method that will prevent disclosure of contents or reconstruction of the document.

For unclassified, unlimited documents, destroy when the report is no longer needed. Do not return it to the originator.

REPORT DOCUMENTATION PAGE

Form Approved
OMB No. 0704-0188

1. AGENCY USE ONLY (Leave blank)	2. REPORT DATE	3. REPORT TYPE AND DATES COVERED
	February 1995	Final

4. TITLE AND SUBTITLE
TRANSLAMINAR FRACTURE TOUGHNESS TEST METHODS AND RESULTS FROM INTERLABORATORY TESTS OF CARBON/EPOXY LAMINATES

5. FUNDING NUMBERS
AMCMS No. 6111.02.H611.1

6. AUTHOR(S)
John H. Underwood, Mark T. Kortschot (U. of Toronto), W. Randolph Lloyd (Idaho Natl. Engineering Lab), Harvey L. Eidinoff (Northrup-Grumman Corp., Bethpage, NY), Dale A. Wilson (Tennessee Tech. U.), and Noel Ashbaugh (U. of Dayton)

7. PERFORMING ORGANIZATION NAME(S) AND ADDRESS(ES)
U.S. Army ARDEC
Benet Laboratories, AMSTA-AR-CCB-O
Watervliet, NY 12189-4050

8. PERFORMING ORGANIZATION REPORT NUMBER
ARCCB-TR-95013

9. SPONSORING / MONITORING AGENCY NAME(S) AND ADDRESS(ES)
U.S. Army ARDEC
Close Combat Armaments Center
Picatinny Arsenal, NJ 07806-5000

10. SPONSORING / MONITORING AGENCY REPORT NUMBER

11. SUPPLEMENTARY NOTES
Presented at the 26th ASTM National Symposium on Fracture Mechanics, Idaho Falls, ID, 27-29 June 1994.
Published in Proceedings of the Conference.

12a. DISTRIBUTION / AVAILABILITY STATEMENT
Approved for public release; distribution unlimited.

12b. DISTRIBUTION CODE

13. ABSTRACT *(Maximum 200 words)*
Fracture tests were performed with carbon/polymer laminates and analyzed for the purpose of developing translaminar fracture toughness test and analysis procedures. Notched specimens were tested on two types of symmetrical layups, quasi-isotropic [0/45/90] and [0/90]; two carbon fiber/epoxy materials, a relatively brittle T300 fiber/976 epoxy and a tougher AS4 fiber/977-2 epoxy; two laminate thicknesses, 2-mm and 4-mm; and three specimen configurations, the standard three-point bend and compact configurations, and an extended compact specimen with arm height-to-specimen width ratio of 1.9. Stress and displacement expressions were obtained for the extended compact specimen, including those for stress intensity factor, K, and crack-mouth opening displacement, V, in terms of relative notch length, a/W, and for a/W in terms of V. Relationships for the bending stresses that control self-similar and off-axis cracking for the extended compact specimen were also derived.

Damage was characterized in the tests, including that associated with arm breakage in the standard compact specimen and load-point damage in the bend specimen. Two types of notch-tip damage were characterized using radiography, that which extends perpendicular to the notch in predominantly 0° fiber layups, and that which occurs ahead of the notch in quasi-isotropic and 90° fiber layups. The applied K at maximum load, K_{max}, determined in a way that took account of the effective crack growth up to the maximum load point, was used as a measure of fracture toughness. For deviations from the linear P-V plot corresponding to $\Delta a/W \leq 0.04$, K_{max} gave consistent measurements of fracture toughness. This criterion also excluded tests with damage of the type that violates the basic concept of fracture toughness measurement, including the arm breakage and load-point damage noted in the tests. Plots of K_{max} versus $\Delta a/W$ showed increasing resistance to crack growth for quasi-isotropic layups and constant resistance to crack growth for predominantly 90° fiber layups.

14. SUBJECT TERMS
Fracture Toughness, Laminated Composites, Carbon/Epoxy, Notch-Tip Damage, X-ray Radiography, Translaminar Fracture, Specimen Configuration

15. NUMBER OF PAGES
25

16. PRICE CODE

17. SECURITY CLASSIFICATION OF REPORT	18. SECURITY CLASSIFICATION OF THIS PAGE	19. SECURITY CLASSIFICATION OF ABSTRACT	20. LIMITATION OF ABSTRACT
UNCLASSIFIED	UNCLASSIFIED	UNCLASSIFIED	UL

TABLE OF CONTENTS

TABLES

LIST OF ILLUSTRATIONS

ACKNOWLEDGEMENTS

We are pleased to acknowledge the help of D. Crayon of the Army Armament Research, Development, and Engineering Center in the performance of much of the testing in this program, and of J. C. Newman, Jr. of NASA Langley Research Center, Dahlgren, VA, for reading the manuscript and providing the K and displacement results of Figure 2.

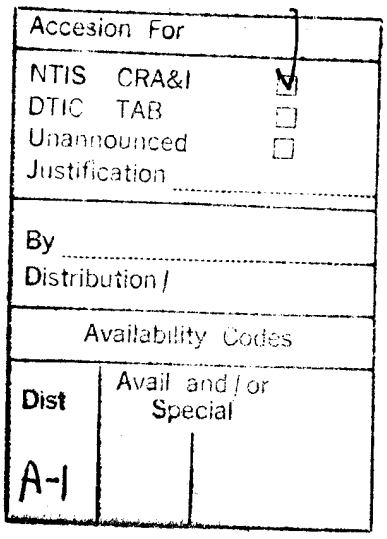

INTRODUCTION

The definitive research on the development of translaminar fracture toughness test methods for carbon/epoxy laminates is the work of Harris and Morris (refs 1,2). They performed load versus crack-opening displacement experiments, notch-tip damage characterization, and finite element K analysis for a wide variety of notched, carbon/epoxy, cross-ply specimens. They observed consistent values of fracture toughness and similar types of damage in center-notched, compact, and three-point bend specimens of varying thickness. Their work addressed the translaminar fracture behavior of laminates with through-thickness defects, as opposed to the more common concern with interlaminar fracture of composite laminates. Interlaminar fracture toughness has received considerably more attention, because of the inherent weakness of delamination compared with through-thickness fracture of a cross-ply laminate. The work of O'Brien et al. (ref 3) describes one part of the extensive development of interlaminar fracture toughness test methods.

There are, however, situations in which through-thickness translaminar fracture is of concern with laminates. Battlefield damage to composite structures can be through-thickness, as can inadvertent projectile impact with commercial aircraft structures. The use of laminates with too few cross-plies is another situation in which translaminar fracture is important. Recent work by some of the current authors and others has addressed the development of translaminar fracture toughness tests, using the work of Harris and Morris (refs 1,2) as a guide. Center-notched panels of two carbon/polymer laminates (ref 4) gave consistent values of fracture toughness in tests with a relatively brittle matrix or with a significant portion of cross-ply fibers. For a tougher matrix or with predominantly 0° fibers, splitting perpendicular to the notch line caused a significant increase in the apparent fracture toughness. Load versus deflection plots and radiographs of notch-tip damage in compact specimens of a quasi-isotropic carbon/epoxy laminate (ref 5) gave similar results to those of Reference 4. For some tests, limited notch-tip damage and consistent fracture toughness values were observed. For other tests, splitting and extensive damage in a direction perpendicular to the notch and increased apparent toughness values were observed.

The objectives of the work here are to identify a specimen configuration and data analysis methods that produce consistent measurements of fracture toughness for carbon/polymer laminates for a wide range of material and layup conditions. Each of the three specimen configurations that has been used for fracture toughness tests of laminates has its problems. The center-notched panel requires a relatively high load for a given applied K value and a large amount of material. The compact specimen has an inherent weakness in its loading arms, which, as shown in the results here, can be a problem for predominantly 0° fiber laminates. The three-point bend specimen has a loading point in close proximity to the notch tip, which, as shown here, can cause a problem. Regarding data analysis methods, the x-ray characterization of notch-tip damage has been shown to be crucial to understanding the test results, but radiographs are too complex to be made part of a routine test and analysis method. What is needed is a method of analyzing the load-deflection data from the test that gives some of the same damage information without the complexity of radiography. The thorough analysis of several series of load-deflection tests and the associated notch-tip damage from radiographs will be used to identify test configurations and data analysis methods that give simple yet consistent fracture toughness measurements.

PARTICIPANTS AND TEST PLAN

The overall plan of test and analysis was developed as part of the technical committee meetings of ASTM Committee E-8 on Fatigue and Fracture. A number of university, government, and industry laboratories were interested in the topic of translaminar fracture toughness of laminates. The laboratories that could devote the time and resources at the time the tests began are shown in Table 1. These laboratories performed the various tests and analyses described here in a cooperative program, with administrative support from ASTM Committee E-8. The two main tasks were performing the fracture tests and analysis and characterizing the notch-tip damage that accompanies fracture.

Table 1. Laboratory Participants

Laboratory	Participation
Lab 1; Army Armament RD&E Center	• Fracture tests/analysis • Coordination of tests
Lab 2; University of Toronto	• Fracture tests • Damage characterization
Lab 3; Idaho National Engineering Laboratory	• Fracture tests • Damage characterization
Lab 4; Grumman Aerospace	• Fracture tests
Lab 5; Tennessee Technological University	• Fracture tests
Lab 6; University of Dayton Research Institute	• Damage characterization

Materials

The materials tested were T300 carbon fiber/976 epoxy and AS4 carbon fiber/977-2 toughened epoxy, each in two symmetrical [0/45/90] and [0/90] layups, as shown in Table 2. The [0/45/90] layups were selected because of the common usage of quasi-isotropic laminates in composite structures. The $[0_2/90]$ and $[90_2/0]$ layups were selected to investigate the problems that can arise in fracture testing of materials with considerable orthotropy. The laminates were made in the form of a 0.45 m by 0.50 m plate with thickness that varied by up to ±6 percent from the mean values in Table 2. The mean values were used for all calculations.

Table 2. Test Conditions and Elastic Modulus Results

Material/Thickness	Calculated Elastic Modulus, E; GPa		
	Three-Point Bend	Standard Compact	Extended Compact
	( ) - number of tests performed		
T300/976 Laminates:			
$[0/+45/90/-45]_{4s}$; 2.1 mm	54 *(2)*	57 *(2)*	55 *(2)*
$[90/-45/0/+45]_{4s}$; 2.1 mm	47 *(2)*	55 *(4)*	59 *(2)*
$[0/0/90]_{6s}$; 2.4 mm	47 *(1)*	37 *(2)*	45 *(2)*
$[90/90/0]_{6s}$; 2.4 mm	33 *(2)*	32 *(2)*	34 *(2)*
AS4/977-2 Laminates:			
$[0/+45/90/-45]_{4s}$; 4.2 mm	52 *(2)*	60 *(2)*	53 *(2)*
$[90/-45/0/+45]_{4s}$; 4.2 mm	55 *(6)*	58 *(12)*	56 *(2)*
$[0/0/90]_{6s}$; 4.8 mm	45 *(2)*	30 *(5)*	44 *(2)*
$[90/90/0]_{6s}$; 4.8 mm	32 *(3)*	29 *(3)*	34 *(2)*

Specimens

The initial plan was to use the compact and three-point bend specimens for the tests, the same configurations (except for thickness) as those used for many other fracture tests, such as in ASTM "Test Method for Plane-Strain Fracture Toughness of Metallic Materials" (E-399). These configurations are shown in Figure 1. Also shown is the typical notch detail that was used, including the 0.3-mm notch width and the integral knife edges that were machined at the crack mouth. Both of these features are important for consistent results. Notch widths much larger than 0.3 mm would be expected to cause increases in apparent toughness (refs 1, 4). In addition, nonintegral knife edges can introduce errors in the measured crack-mouth displacement and an improper interpretation of test results.

As the work progressed, problems arose with the compact and three-point bend specimens, as will be discussed later. This led to the use of a third specimen configuration, called the extended compact, see Figure 1d. This type of specimen was used by Richardson and Goree (ref 6) in fracture testing and failure modeling of aluminum, using a half-height of the loading arms relative to specimen width, H/W, of 1.2. Recently, Piascik and Newman (ref 7) calculated values of applied stress intensity factor, K, and crack-mouth displacement, V, for an extended compact specimen with H/W = 1.9, the configuration chosen for use here. Note that in addition to the different H/W compared with the standard compact specimen, the extended compact has different definitions of W and a, the notch length. W is the full width of the specimen and a is measured from the edge of the specimen. A summary of the number of tests performed with each type of specimen is given in Table 2.

K AND DISPLACEMENT EXPRESSIONS

Accurate, wide-range expressions for elastic K and V in terms of load, P, and specimen dimensions and a/W in terms of P and V are needed for analysis of the P versus V plots. For the standard compact and bend specimens this information is readily available, since it is commonly used in various fracture tests. For the extended compact specimen, basic elastic stress analysis results (ref 7) are used here to develop new expressions. It is recognized that the K and V expressions should account for the anisotropic nature of laminates. This was considered to be beyond the scope of this work and is the subject of a continuing effort.

Three-Point Bend Specimen

The dimensionless applied stress intensity factor, $KBW^{1/2}/P$, is (ref 8)

$$KBW^{1/2}/P = [3\,\alpha^{1/2}\,S/W]\,[1.99 - \alpha(1-\alpha)(2.15 - 3.93\,\alpha + 2.7\,\alpha^2)/2(1+2\alpha)(1-\alpha)^{3/2}]$$

$$\text{for } 0 \le \alpha \le 1 \text{ and } S/W = 4 \qquad (1)$$

where B is thickness, S is span, and $\alpha = a/W$, relative notch depth. The dimensionless elastic crack-mouth displacement, VEB/P, is (ref 9)

$$VEB/P = [6\,\alpha\,S/W]\,[0.76 - 2.28\,\alpha + 3.87\,\alpha^2 - 2.04\,\alpha^3 + 0.66/(1-\alpha)^2]$$

$$\text{for } 0 \le \alpha \le 1 \text{ and } S/W = 4 \qquad (2)$$

where E is elastic modulus. The inverse of Eq. (2), giving α in terms of VEB/P (ref 10), is

$$\alpha = 0.999748 - 3.9504\,u + 2.9821\,u^2 - 3.21408\,u^3 + 51.51564\,u^4 - 113.031\,u^5$$

$$\text{for } u = 1/[(VEB/P)^{1/2} + 1] \text{ and } 0.2 \le \alpha \le 1 \qquad (3)$$

Standard Compact Specimen

The $KBW^{1/2}/P$ expression is (ref 8)

$$KBW^{1/2}/P = [2+\alpha]\,[0.886 + 4.64\,\alpha - 13.32\,\alpha^2 + 14.72\,\alpha^3 - 5.6\,\alpha^4]/[1-\alpha]^{3/2}$$

$$\text{for } 0.2 \le \alpha \le 1 \qquad (4)$$

The VEB/P expression is (ref 11)

$$VEB/P = [1+\alpha]^2\,[2.163 + 12.219\,\alpha - 20.065\,\alpha^2 - 0.9925\,\alpha^3 + 20.609\,\alpha^4 - 9.9314\,\alpha^5]/[1-\alpha]^2$$

$$\text{for } 0.2 \le \alpha \le 1 \qquad (5)$$

The α expression is (ref 12)

$$\alpha = 1.000196 - 4.06319\,u + 11.242\,u^2 - 106.043\,u^3 + 464.335\,u^4 - 650.677\,u^5$$

$$\text{for } u = 1/[(VEB/P)^{1/2} + 1] \text{ and } 0.2 \le \alpha \le 1 \qquad (6)$$

Extended Compact Specimen

Recent numerical results (ref 7) provide the basis for K and displacement expressions for the extended compact specimen. The results for the configuration shown in Figure 1d are summarized in Table 3. These results were used here to obtain expressions in the same form as Eqs. (1) through (6), above, using regression analysis and also fitting to the shallow and deep crack-limit solutions as in recent work (ref 13). The resulting K expression is

$$KBW^{1/2}/P = \alpha^{1/2}\,[1.4 + \alpha]\,[3.97 - 10.88\,\alpha + 26.25\,\alpha^2 - 38.9\,\alpha^3 + 30.15\,\alpha^4 - 9.27\,\alpha^5]/[1-\alpha]^{3/2}$$

$$\text{for } 0 \le \alpha \le 1 \qquad (7)$$

Equation (7) fits the numerical results and the limits within 0.4 percent, except for the numerical results at the two extremes (a/W = 0 and 0.92), which are 0.9 percent below and 0.7 percent above the values from Eq.(7), respectively. The VEB/P expression is

$$VEB/P = [15.52\,\alpha - 26.38\,\alpha^2 + 49.70\,\alpha^3 - 40.74\,\alpha^4 + 14.44\,\alpha^5]/[1-\alpha]^2$$

$$\text{for } 0 \le \alpha \le 1 \qquad (8)$$

which fits the numerical results and the limits within 0.3 percent, except for a/W = 0.92 where the numerical result is 0.7 percent above the value from Eq. (8). The inverse of Eq. (8) is

$$\alpha = 1.0004 - 3.5495\,u + 6.0988\,u^2 - 16.0075\,u^3 + 32.3436\,u^4 - 22.2843\,u^5$$

$$\text{for } u = 1/[(VEB/P)^{1/2} + 1] \text{ and } 0.15 \le \alpha \le 1 \qquad (9)$$

Equation (9) fits the numerical results and the deep crack limit within 0.04 percent over the range $0.15 \le \alpha \le 1$.

Table 3. K and Displacement Results for Extended Compact Specimen

a/W	$KBW^{1/2}/P$	VEB/P
0.100	1.721	1.664
0.150	2.155	2.622
0.200	2.586	3.750
0.250	3.049	5.127
0.300	3.571	6.853
0.350	4.178	9.072
0.400	4.904	11.990
0.450	5.792	15.910
0.500	6.907	21.330
0.550	8.343	29.020
0.600	10.250	40.300
0.650	12.880	57.580
0.700	16.670	85.510
0.725	19.240	106.200
0.750	22.480	134.100
0.775	26.660	172.600
0.800	32.210	227.600
0.825	39.840	309.700
0.840	45.950	379.500
0.920	136.400	1743.000

The numerical results for $KBW^{1/2}/P$ and VEB/P are compared with Eqs. (7) and (8) in Figure 2. Note that functions of a/W derived from the shallow and deep crack K and V limits have been used in the plot, in order to obtain finite values over the entire range of a/W. It is clear that the numerical results and the fitted expressions are well behaved and properly approach the known, exact limits.

Notch-Tip Stresses

The notch-tip splitting and damage that extends off the axis of the notch, discussed earlier, occurs in compact specimen tests of other materials (ref 14). In Reference 14 calculations of the nominal bending stress in two directions at the notch tip were made which showed why off-axis splitting occurred in standard compact specimens and did not occur in bend specimens. These calculations are summarized as follows. For the standard compact specimen

$$S_Y W^{1/2}/K = 3(1+\alpha)/f_C (1-\alpha)^2 \quad (10)$$

$$S_X W^{1/2}/K = 16.67\ \alpha/f_C \quad (11)$$

where S_Y and S_X are the nominal, notch-tip bending stresses that control self-similar and off-axis cracking, respectively, and $f_C = KBW^{1/2}/P$ for the compact specimen. For the bend specimen

$$S_Y W^{1/2}/K = 1.5/f_B (1-\alpha)^2 \quad (12)$$

$$S_X W^{1/2}/K = 0.375/f_B \quad (13)$$

where $f_B = KBW^{1/2}/P$ for the bend specimen.

Similar calculations were made here for the extended compact specimen, as follows, referring also to Figure 3. The expression

$$S_Y = 6\ M/B\ (W-a)^2 \quad (14)$$

gives the y-direction nominal bending stress that drives self-similar cracking from the notch, where the applied moment, M, is

$$M = P[a - 0.2\ W + (W-a)/2] \quad (15)$$

Combining Eqs. (14), (15), and (7) gives

$$S_Y W^{1/2}/K = 3(0.6 + \alpha)/f_E (1-\alpha)^2 \quad (16)$$

where, as before, $f_E = KBW^{1/2}/P$, from Eq. (7) in this case. For the x-direction bending stress that drives off-axis cracking

$$S_X = 6\ M/B\ H^2 \text{ and} \quad (17)$$

$$M = 6\ P\ (a - 0.2\ W) \quad (18)$$

and the result is

$$S_X W^{1/2}/K = 16.67\ (\alpha - 0.2)/f_E \quad (19)$$

Equations (10) through (13), (16), and (19) are plotted in Figure 3. They compare the bending stresses that control self-similar and off-axis cracking for the three specimen configurations. The plot of $SW^{1/2}/K$ provides a dimensionless comparison of these important bending stresses at any given applied K level and for a range of a/W. For the standard compact specimen at relatively small a/W, the off-axis bending stress approaches the same magnitude as that for self-similar cracking. This explains the off-axis cracking problems with this specimen. Note that this problem is not expected for the extended compact specimen, nor for the three-point bend specimen. The large dimensions of these specimen configurations in the direction perpendicular to the notch reduces the bending stress, S_x (also referred to as the T-stress), that drives off-axis cracking, so that this type of cracking does not occur.

RESULTS AND DISCUSSION

Load-Displacement and Modulus

Load versus crack-mouth displacement tests were performed for each of the twenty-four test conditions summarized in Table 2, that is, for each of the three specimen configurations and the eight laminates. Figures 4 and 5 show the measured loads and displacements for the AS4/977-2 material in [0/0/90] layup and the T300/976 material in [90/-45/0/+45] layup, respectively. The types of load-displacement behavior shown in Figures 4 and 5 are the two general types noted in the tests, a predominantly nonlinear P-V plot with an early and significant deviation from initial linearity, and a predominantly linear plot with just a few nearly linear unloading and reloading segments. The nonlinear plots were typically from specimens with more 0° fibers and those made of the AS4/977-2 material. Note in Figure 4 that the extremely nonlinear P-V plot from a [0/0/90] standard compact specimen was associated with a splitting failure of the specimen arm in a direction perpendicular to the notch axis.

For all tests an accurate measurement of the initial linear slope was possible. Using the slope, the initial notch depths, and Eqs. (2), (5), and (8), calculations of elastic modulus were made and listed in Table 2. In general, the measured modulus was in the expected range (ref 1). Also of interest are the differences in measured modulus for certain combinations of specimen configuration and layup. Note the relatively low E values for the [0/0/90] standard compact tests. The low E may be an indication of an imminent splitting-type of arm failure, discussed above, since it occurred with the same combination of configuration and layup. Note one other relatively low E value, that for the [90/-45/0/+45] T300/976 three-point bend tests. This low E value is believed to be due to the type of damage that occurs ahead of the notch in the three-point bend specimen, discussed next.

Notch-Tip Damage

A potential problem with the close proximity of the middle load point and the notch tip in the three-point bend specimen was noted during testing. Damage could be seen by the unaided eye around the load point. To investigate this further, specimens were unloaded just after the maximum load had been attained and inspected for notch-tip and load-point damage using an ultrasonic test method. A through-transmission attenuation method was used that scanned the unloaded specimens. Figure 6 shows results for two layups of the AS4/977-2 material. The [90/90/0] specimen shows a quite well developed notch-tip damage zone and no evidence of damage at the load point, whereas the [90/-45/0/+45] specimen, with a smaller notch-tip damage zone, shows considerable load-point damage. It is clear that, for some layups, the three-point bend specimen is inadvisable for use in fracture toughness testing.

The arm failure problem with the standard compact specimen and the load-point problem with the three-point bend specimen led to the interest in the extended compact specimen. Characterization of the notch-tip damage zone development and any significant load-point damage with the extended compact specimen was performed using the x-ray infiltration method (ref 15). Specimens of each of the eight material and layup

combinations in Table 2 were unloaded just after maximum load had been attained and inspected by radiography. Selected results are shown in Figures 7 and 8. The only damage noted in all samples was associated with the notch. No damage was observed at the holes. However, had a layup been tested with more than a 2:1 ratio of 0° to 90° fibers, hole pullout might have been experienced.

The AS4/977-2 results in Figure 7 are interpreted as a damage zone extending primarily ahead of the notch tip for the [90/-45/0/+45] layup (with very similar results for the [0/+45/90/-45] layup, not shown); a zone extending perpendicular to the notch by splitting along the 0° fibers for the [0/0/90] layup; an intense zone and effective crack growth occurring directly ahead of the notch and lesser damage extending perpendicular to the notch for the [90/90/0] layup.

The T300/976 results in Figure 8 are similar in general nature to those in Figure 7, but with larger damage zones and more effective crack growth because the more brittle T300/976 material sustained more damage before the unloading could be accomplished. The [90/-45/0/+45] layup zone extends primarily ahead of the notch, as with the other material, but an intense damage zone and effective cracking directly ahead of the notch can also be seen. The [0/0/90] zone extends perpendicular to the notch, as with the other material, but intense damage directly ahead of the notch can also be seen. The [90/90/0] damage zone is dominated by intense damage directly ahead of the notch, with significant damage perpendicular to the notch occurring in only two locations. These locations are believed to correspond to specific linear segments of the P-V curve, of the type shown in Figure 5.

In summary, the infiltration radiographs showed damage extending ahead of the notch and, for layups with a significant portion of 0° fibers, damage extending perpendicular to the notch. As the damage zone grows, an area of intense damage directly ahead of the notch occurs that is associated with effective through-thickness crack growth ahead of the notch. The extension of damage ahead of the notch tip was measured from the radiographs for fifteen extended compact specimens (the unloading of one specimen was not quick enough). Comparison of these measurements of effective crack growth with calculations of crack growth based on the P-V plots is presented next.

Calculated Crack Growth

Calculations of crack growth were made from the unloading slope of the P-V plots, using Eqs. (3), (6), and (9) and the E values determined from the loading slope. These calculations are compared in Figure 9 with the measured full extent of the damage zone from radiographs taken after unloading, such as those in Figures 7 and 8. In prior work (ref 5) with standard compact specimens of the same AS4/977-2 [0/+45/90/-45] laminate used here, the unloading slope calculation of crack growth was found to correspond to about 80 percent of the full extent of the radiographic damage zone. In Figure 9 the regression line indicates that unloading slope crack growth averages 76 percent of the full extent of the radiographic damage zone. Thus, the results for extended compact specimens of two materials and various layups show a similar close relationship between unloading-slope crack growth and damage zone, as was the case in the prior work.

Additional crack growth calculations were made just beyond the P_{max} point in the test, based on the additional increment of crack-mouth-displacement, ΔV, beyond the initial linear P-V plot, V_o, see Figure 5. The calculation was made by modifying Eq. (9) with a different expression for u, as follows:

$$u_{max} = 1/[(V_o\, EB/P_{max} + \Delta V\, EB/P_{max})^{1/2} + 1] \qquad (20)$$

where u_{max} corresponds to the total relative notch-plus-crack length at P_{max}, *including* the crack growth associated with ΔV. Combining Eq. (20) with (9) (or with the appropriate expressions for the other specimen configurations) gives a method to calculate elastic crack growth at P_{max}. For P-V plots such as those in

Figure 5, with displacements that are predominantly elastic, this calculation is appropriate. For plots such as those in Figure 4, comparison of results may indicate whether or not it is appropriate. A comparison of crack growth calculated using ΔV (Eq. 20) with that using the unloading slope just after P_{max} (Eqs. 3,6,9) is shown in Figure 10, for all tests for which both calculations were possible. The two calculations are in good agreement, as shown by the regression line lying close to the dashed line that indicates perfect agreement. Since the crack growth calculated from the ΔV value at P_{max} does not require an unloading at a specific point, it is the more useful determination of crack growth in assessments of fracture toughness, discussed next.

Fracture Toughness

Two calculations of the applied K value at the maximum load point were made, as prospective fracture toughness determinations from the tests, designated $K_{max\text{-}o}$ and K_{max}. The calculations were made using Eqs. (1), (4), and (7) as appropriate and using α_o, the a/W of the machined notch, and α_v, the a/W of the notch plus the crack growth calculated using Eq. (20). Table 4 summarizes the calculations for the specimens of Figure 5. Note that K_{max}, which includes the ΔV calculation of crack growth, is considerably higher than $K_{max\text{-}o}$, 37 percent higher for the extended compact specimen. The summary of all the $K_{max\text{-}o}$ and K_{max} results may indicate which is the better measure of fracture toughness.

Table 4. Typical Spread Sheet Calculations for T300/976 [90/-45/0/45] Layup Specimens Shown in Figure 5

Specimen	α_o	P_{max}	$K_{max\text{-}o}$	ΔV	α_v	K_{max}
		KN	MPa$\sqrt{m}$	mm		MPa$\sqrt{m}$
	Test	Test	Eq. 1,4,7	Test	Eq. 20	Eq. 1,4,7
Three-Point Bend	0.480	1.10	33.4	0.11	0.531	39.3
Std. Compact	0.490	1.05	29.3	0.09	0.527	32.9
Ext. Compact	0.508	1.58	32.2	0.15	0.575	44.1

Figures 11 and 12 show the mean values of $K_{max\text{-}o}$ and K_{max} for the test conditions listed in Table 2. Examples of the variability of the results are eight AS4/977-2 [90/+45/0/-45] tests (from two labs) that gave mean and standard error $K_{max\text{-}o}$ values of 56.6 and 2.9 MPa$\sqrt{m}$ and mean and standard error K_{max} values of 61.3 and 4.0 MPa$\sqrt{m}$. The largest difference between $K_{max\text{-}o}$ and K_{max} for both material types was noted for standard compact specimens with the [0/0/90] layup. This is attributed to the arm breakage problem which occurred with this specimen-layup combination. In general, the more brittle T300/976 material showed less difference between $K_{max\text{-}o}$ and K_{max} than the AS4/977-2 material; this is consistent with less crack growth at P_{max} for the more brittle material. For the extended compact results, which are not affected by either arm breakage or load-point damage, the value of K_{max} averages 12 percent above $K_{max\text{-}o}$. Particularly the last two observations suggest that the difference between $K_{max\text{-}o}$ and K_{max} is real and is due to an increasing crack growth resistance curve for at least some of the material and layup combinations of these tests. A similar observation was made in the prior work (ref 5).

Additional evidence of increasing crack growth resistance behavior can be seen in Figure 13, a plot of K_{max} versus calculated crack growth at maximum load (using Eq. 20). Note that each point on the plot is a separate test, so that taken together the results for a given material and layup combination describe the general crack growth resistance for that type of laminate. Three definitive types of behavior were noted (with specimens of each of the three configurations) and illustrated using linear regression lines. For the AS4/977-2 material in [0/+45/90/-45] and [90/-45/0/+45] layups, a relatively steeply rising K-R curve was seen, whereas for the T300/976 material in [0/+45/90/-45] and [90/-45/0/+45] layups, a less steeply rising K-R curve was seen. For the AS4/977-2 material in [90/90/0] layup, a nearly horizontal K-R curve was noted. These three types of behavior are rationalized as follows: the AS4 0/45/90 layups, having a tough matrix and quasi-isotropic properties, have significant fiber bridging and thus a steeply rising K-R curve; the T300 0/45/90 layups, although quasi-isotropic, have a less tough matrix and thus less bridging and a less steeply rising K-R curve; the AS4 90/90/0 layup is dominated by the 90° fibers aligned with the crack growth direction which prevent fiber bridging and any rising K-R curve behavior.

One other set of results is plotted in Figure 13 for the AS4 0/0/90 layup tests. No trend of these results was considered because of the problems with the bend and compact specimens discussed earlier. These problems may have caused low K_{max} values for the AS4 0/0/90 bend and standard compact tests (indicated with B and C in the plot), compared with the extended compact tests. Other T300 test results were so closely grouped that no significant K-R curve trends were apparent.

The consistent trends of K-R behavior noted in Figure 13 were determined from elastic calculations of crack growth based on the ΔV of the P-V plot. This suggests that a series of $\Delta a/W$ versus $\Delta V/V_o$ curves can be drawn for different specimen configurations and starting crack lengths, as shown in Figure 14. The curves were calculated using Eq. (20) with Eqs. (3) and (9), by assuming values of $\Delta V/V_o$ and calculating the $\Delta a/W$ that would have caused those values of $\Delta V/V_o$. The plots of Figure 14 can be used with the summary of K_{max} versus $\Delta a/W$ results in Figure 13 to propose a simple criterion for determining fracture toughness from a P-V plot of a carbon/epoxy specimen. From Figure 13, the preponderance of results has $\Delta a/W$ values of 0 to 0.04; for the extended compact specimen, this corresponds to $\Delta V/V_o$ of 0 to 0.3. This is proposed as the basis of fracture toughness determination for these types of carbon/epoxy laminates, as follows. The extended compact specimen is used with a starting a/W between 0.5 and 0.6; P versus V is recorded and K_{max} is calculated from Eqs. (7), (9), and (20); K_{max} gives a measure of fracture toughness provided that $\Delta V/V_o \leq 0.3$. This determination of fracture toughness would give consistent results for the tests here. It would also exclude the tests affected by whole-specimen and notch-tip damage uncharacteristic of the self-similar crack growth that must dominate a determination of fracture toughness. The $\Delta V/V_o \leq 0.3$ criterion would exclude tests with the arm breakage damage of the standard compact specimen, the load-point damage of the bend specimen, and the damage extending perpendicular to the notch for all tests of layups with a significant portion of 0° fibers.

SUMMARY

Fracture tests were performed with carbon/polymer laminates and analyzed for the purpose of developing translaminar fracture toughness test and analysis procedures. Notched specimens were tested of two types of symmetrical layups, quasi-isotropic [0/45/90] and [0/90]; two carbon fiber/epoxy materials, a relatively brittle T300 fiber/976 epoxy and a tougher AS4 fiber/977-2 epoxy; two laminate thicknesses, 2 mm and 4 mm; and three specimen configurations, the standard three-point bend and compact configurations used for many types of fracture tests, and an extended compact specimen with arm height-to-specimen width ratio of 1.9, compared to 0.6 for the standard compact specimen. Plots of load versus crack-mouth opening displacement were obtained and analyzed to determine the progression of crack growth and damage during the test.

Wide-range stress and displacement expressions were obtained for the extended compact specimen. Expressions for applied stress intensity factor, K, and crack-mouth opening displacement, V, in terms of relative notch length, a/W, and for a/W in terms of V were developed from recent numerical results. Relationships for the nominal bending stresses that control both self-similar and off-axis cracking for the extended compact specimen were derived and used to explain the types of cracking observed.

Damage that was unrelated to crack growth from the notch tip was characterized in the tests, including the damage associated with the arm breakage problem with the standard compact specimen and the load-point damage with the three-point bend specimen. Notch-tip damage of two types was characterized using radiography: damage that extends primarily perpendicular to the notch in predominantly 0° fiber layups associated with high toughness, and damage that extends primarily ahead of the notch in quasi-isotropic and predominantly 90° fiber layups associated with lower toughness. Elastic calculations of crack extension from the notch tip averaged 76 percent of the extent of radiographic notch-tip damage zone.

The applied K at maximum load, K_{max}, including the effect of the crack growth up to the maximum load point, was used as a measure of fracture toughness. Imminent arm breakage with the standard compact specimen and load-point damage with the bend specimen adversely affected the measurement of K_{max}, causing significant decreases. Plots of K_{max} versus crack growth unaffected by adverse damage showed an increasing resistance to crack growth for quasi-isotropic layups and a constant resistance to crack growth for predominantly 90° fiber layups. The K_{max} from the extended compact specimen, including the effect of crack growth, was proposed as a measurement of translaminar fracture toughness for carbon/epoxy laminates. For deviations from the linear P-V plot corresponding to $\Delta a/W \leq 0.04$, the K_{max} values gave consistent measurements of fracture toughness. This criterion also excluded tests with damage of the type that violates the concept of fracture toughness measurement.

REFERENCES

1. C.E. Harris and D.H. Morris, "Fracture Behavior of Thick Laminated Graphite/Epoxy Composites," NASA CR-3784, National Aeronautics and Space Administration, Washington, DC, March 1984.

2. C.E. Harris and D.H. Morris, "A Comparison of the Fracture Behavior of Thick Laminated Composites Utilizing Compact Tension, Three-Point Bend and Center-Cracked Tension Specimens," *Fracture Mechanics: Seventeenth Volume, ASTM STP 905*, American Society for Testing and Materials, Philadelphia, 1986, pp. 124-135.

3. T.K. O'Brien, N.J. Johnston, I.S. Raju, D.J. Morris, and R.A. Simonds, "Comparisons of Various Configurations of the Edge Delamination Test for Interlaminar Fracture Toughness," *Toughened Composites, ASTM STP 937*, (N.J. Johnston, Ed.), American Society for Testing and Materials, Philadelphia, 1987, pp. 199-221.

4. J.H. Underwood, I.A. Burch, and S. Bandyopadhyay, "Effects of Notch Geometry and Moisture on Fracture Strength of Carbon/Epoxy and Carbon/Bismaleimide Laminates," *Composite Materials: Fatigue and Fracture (Third Volume), ASTM STP 1110*, (T.K. O'Brien, Ed.), American Society for Testing and Materials, Philadelphia, 1991, pp. 667-685.

5. J.H. Underwood, and M.T. Kortschot, "Notch-Tip Damage and Translaminar Fracture Toughness Measurements from Carbon/Epoxy Laminates," *Proceedings of 2nd International Conference on Deformation and Fracture of Composites*, The Institute of Materials, London, 1993.

6. D.E. Richardson and J.G. Goree, "Experimental Verification of a New Two-Parameter Fracture Model," *Fracture Mechanics: Twenty-Third Symposium, ASTM STP 1189*, (Ravinder Chona, Ed.), American Society for Testing and Materials, Philadelphia, 1993, pp. 738-750.

7. R.S. Piascik, and J.C. Newman, Jr., *International Journal of Fracture*, to be published.

8. J.E. Srawley, "Wide Range Stress Intensity Factor Expressions for ASTM E-399 Standard Fracture Toughness Specimens," *International Journal of Fracture Mechanics*, Vol. 12, June 1976, p. 475.

9. H. Tada, P.C. Paris, and G.R. Irwin, *The Stress Analysis of Cracks Handbook*, Paris Productions, St. Louis, MO, 1985, pp. 2.16-2.18.

10. S.X. Wu, "Crack Length Calculation Formula for Three-Point Bend Specimens," *International Journal of Fracture*, Vol. 24, 1984, pp. R33-R35.

11. W.R. Andrews, G.A. Clark, P.C. Paris, and D.W. Schmidt, "Single Specimen Tests for J_{Ic} Determination," *Mechanics of Crack Growth, ASTM STP 590*, American Society for Testing and Materials, Philadelphia, 1976, pp. 27-32.

12. A. Saxena, and S.J. Hudak, Jr., "Review and Extension of Compliance Information for Common Crack Growth Specimens," *International Journal of Fracture*, Vol. 14, 1978, pp. 453-468.

13. J.H. Underwood, "Stress Intensity Factor and Load-Line Displacement Expressions for the Round Bar Bend Specimen," *International Journal of Fracture*, Vol. 62, 1993, pp. R49-R55.

14. E. Troiano, J.H. Underwood, R.T. Abbott, A.A. Kapusta, and D.E. Leighton, "Fracture Response of Whisker Reinforced SiC/Aluminum Metal Matrix Composite," *Proceedings of ASME Winter Annual Meeting*, American Society of Mechanical Engineers, New York, 1993.

15. M.T. Kortschot and P.W.R. Beaumont, "Damage Mechanics of Composite Materials: I - Measurements of Damage and Strength," *Composites Science and Technology*, Vol. 39, 1990, pp. 289-301.

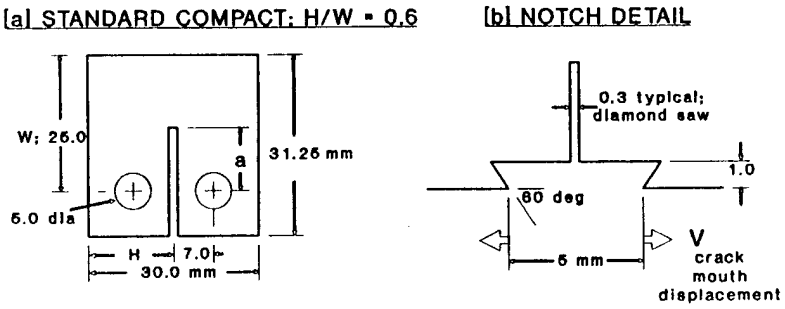

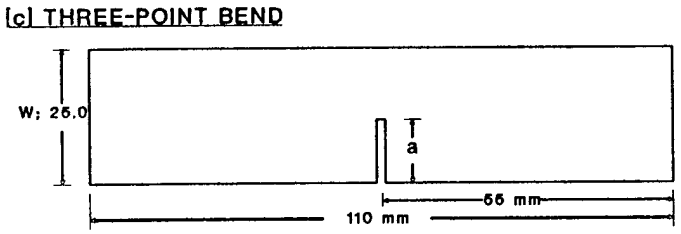

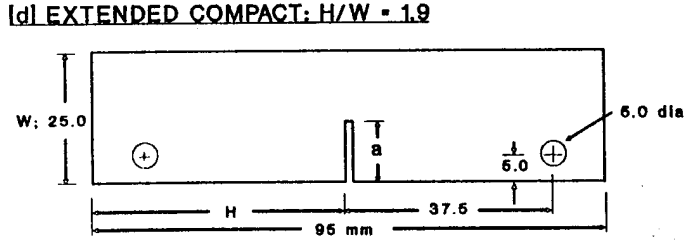

FIG. 1 - *Specimen configurations*

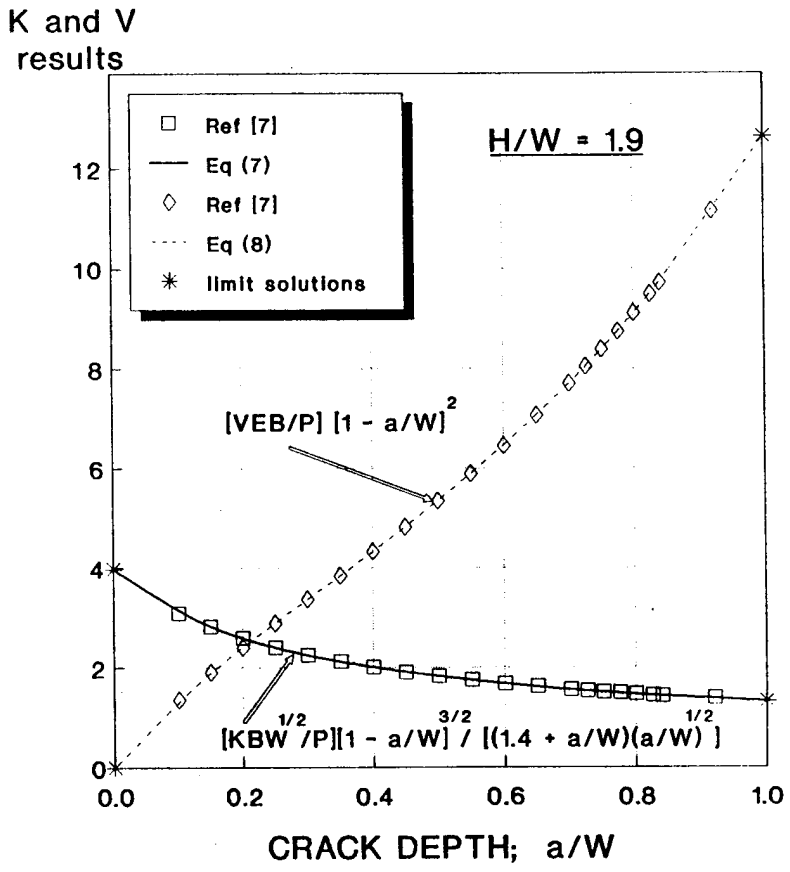

FIG. 2 - *Stress Intensity and displacement results for the extended compact specimen.*

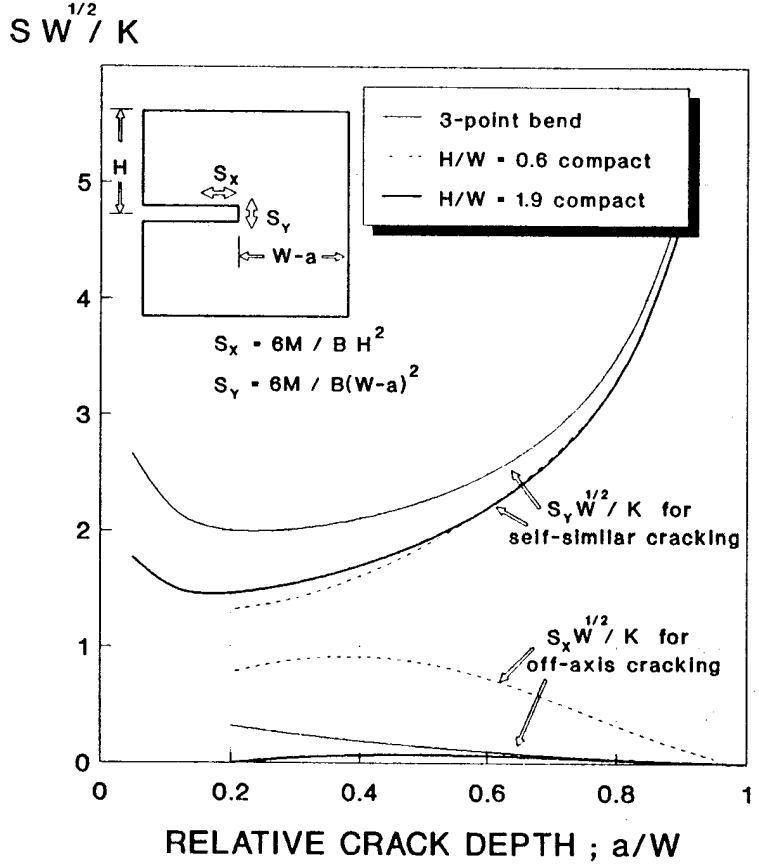

FIG. 3 - *Stresses controlling off-axis and self-similar cracking in bend, compact and extended compact specimens.*

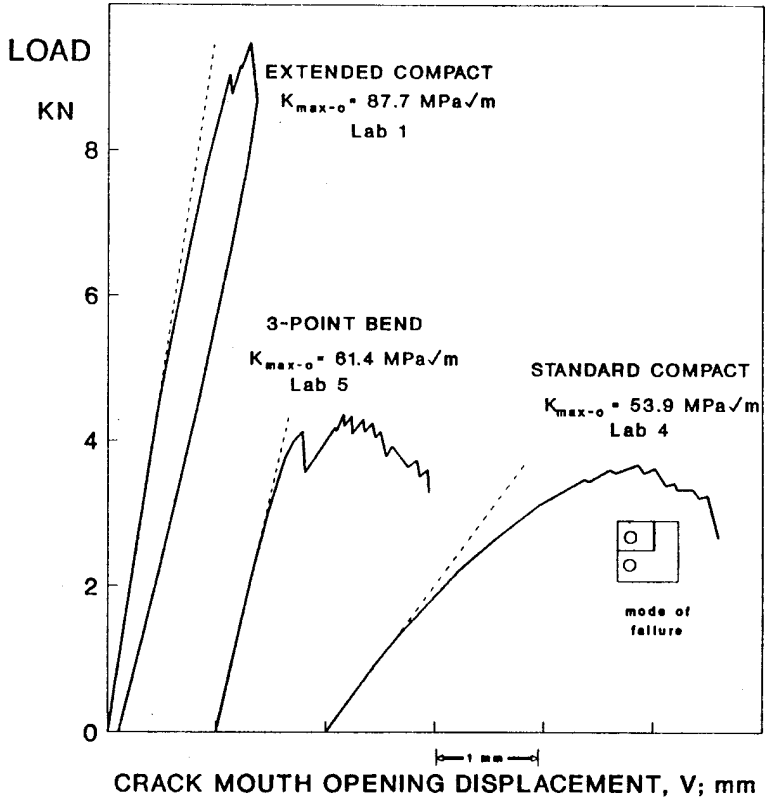

FIG. 4 - *Load vs V for bend, compact and extended compact specimens; AS4/977-2 with [0/0/90] layup*

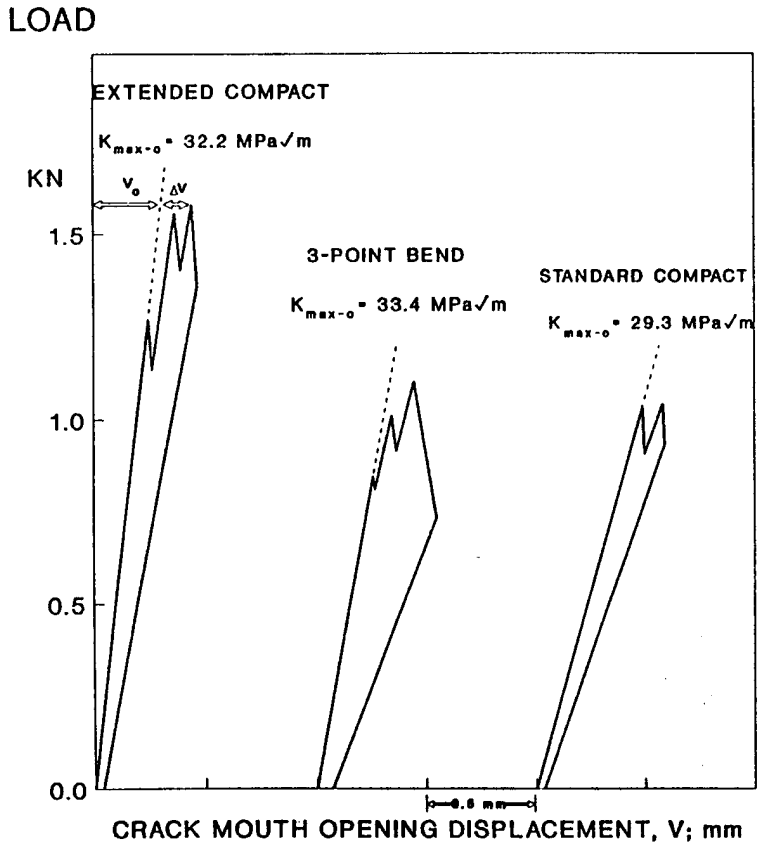

FIG. 5 - *Load vs V for bend, compact and extended compact specimens; T300/976 with [90/-45/0/45] layup*

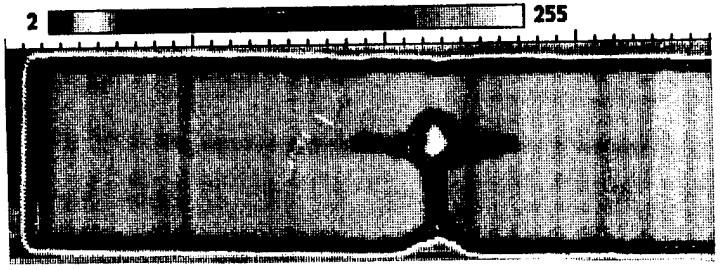

[a] [90/90/0] layup

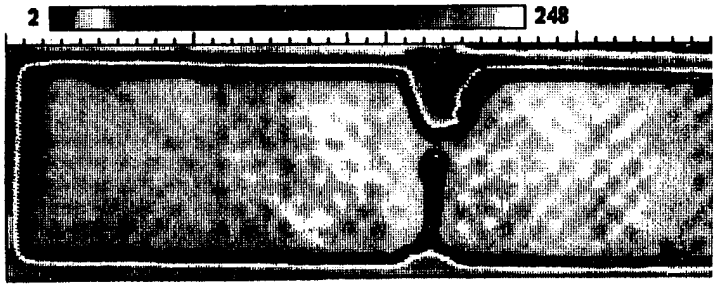

[b] [90/-45/0/+45] layup

FIG. 6 - *Ultrasonic attenuation in notch-tip and load-point damage zones for AS4/977-2 laminates*

[a] [90/-45/0/+45] layup

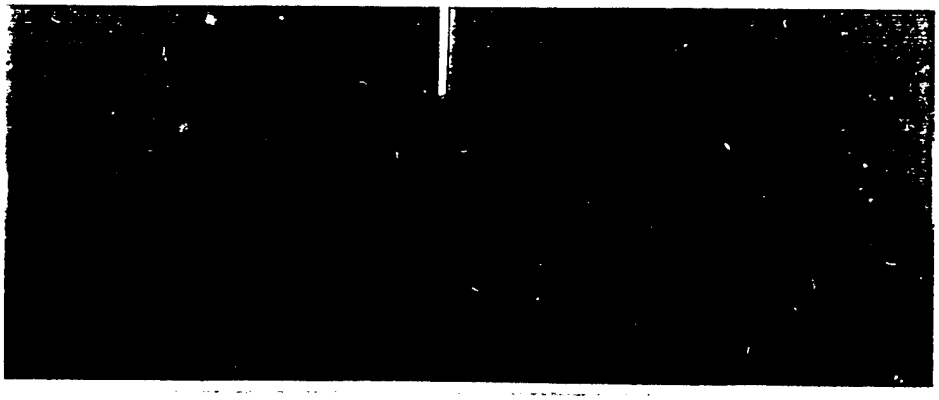

[b] [0/0/90] layup

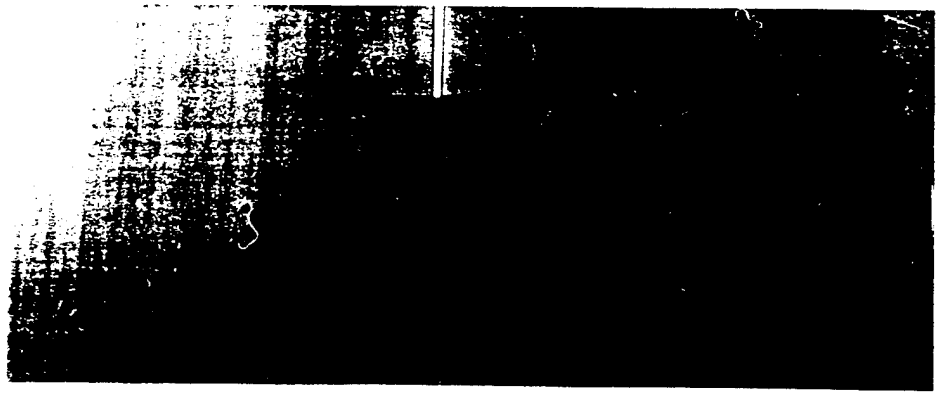

[c] [90/90/0] layup

FIG. 7 - Infiltration radiographs of damage in AS4/977-2 laminates.

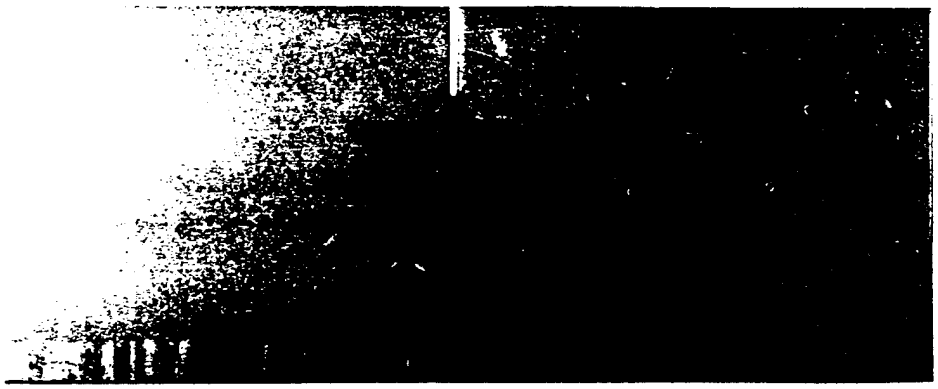

[a] [90/-45/0/+45] layup

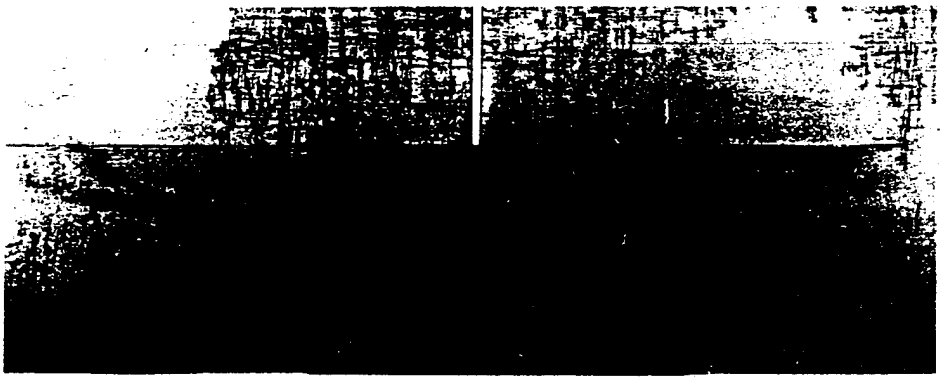

[b] [0/0/90] layup

[c] [90/90/0] layup

FIG. 8 - Infiltration radiographs of damage in T300/976 laminates.

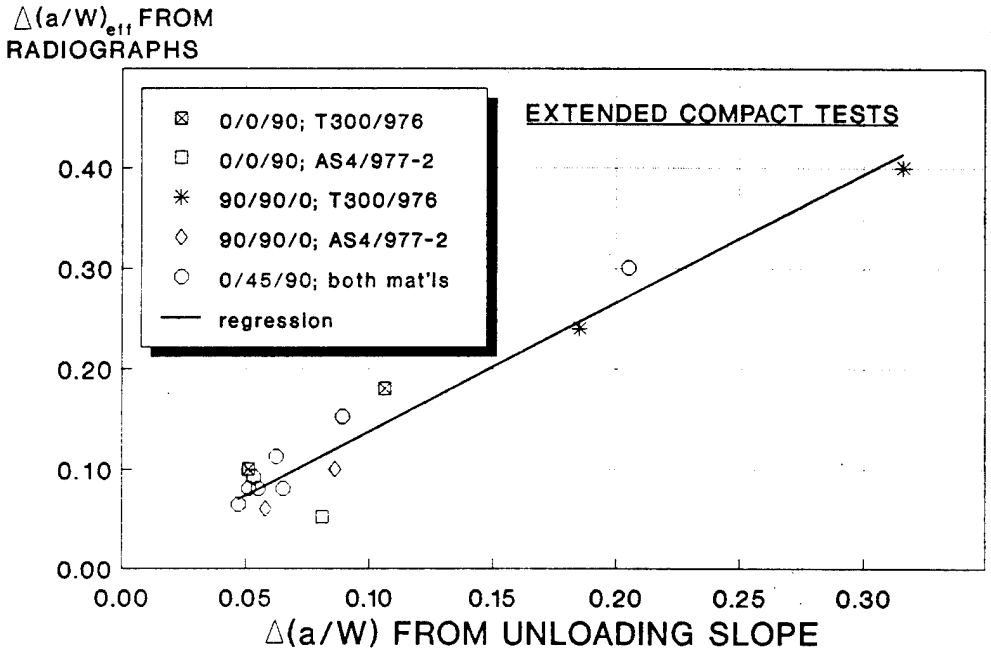

FIG. 9 - *Effective crack growth from radiograph damage versus calculated crack growth from unloading slope.*

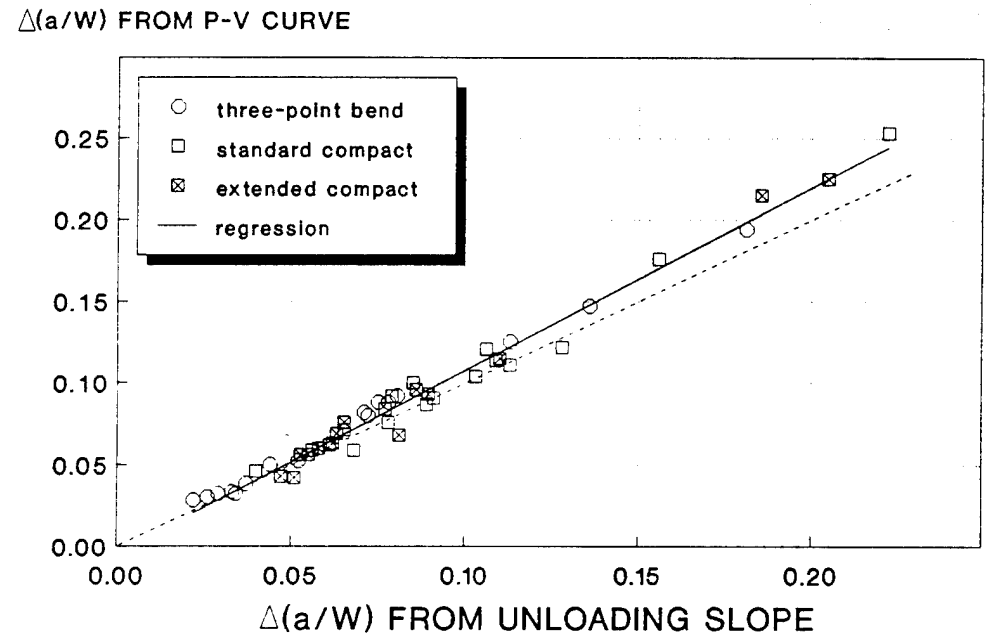

FIG. 10 - *Crack growth calculated from P-V curve compared with crack growth calculated from unloading slope*

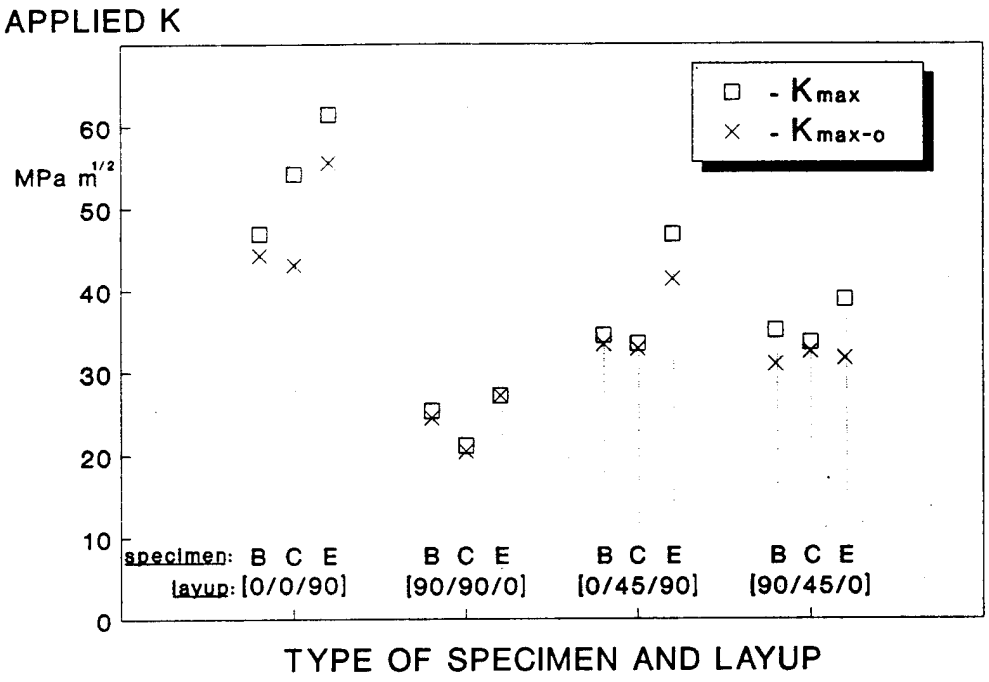

FIG. 11 - *Mean applied K values at maximum load for T300/976 laminates*

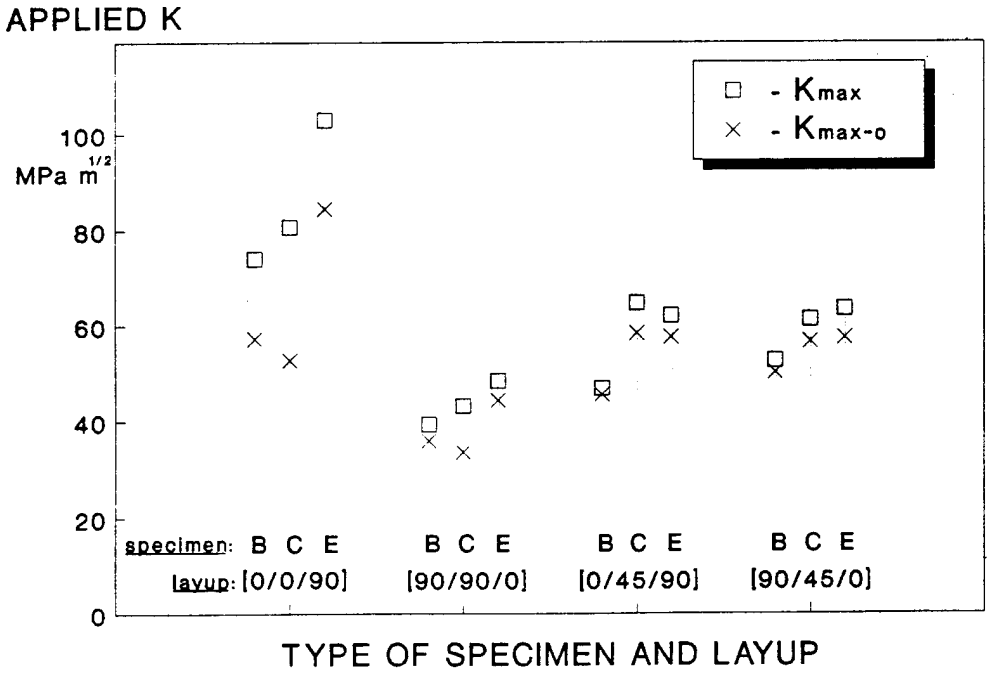

FIG. 12 - *Mean applied K values at maximum load for AS4/977-2 laminates*

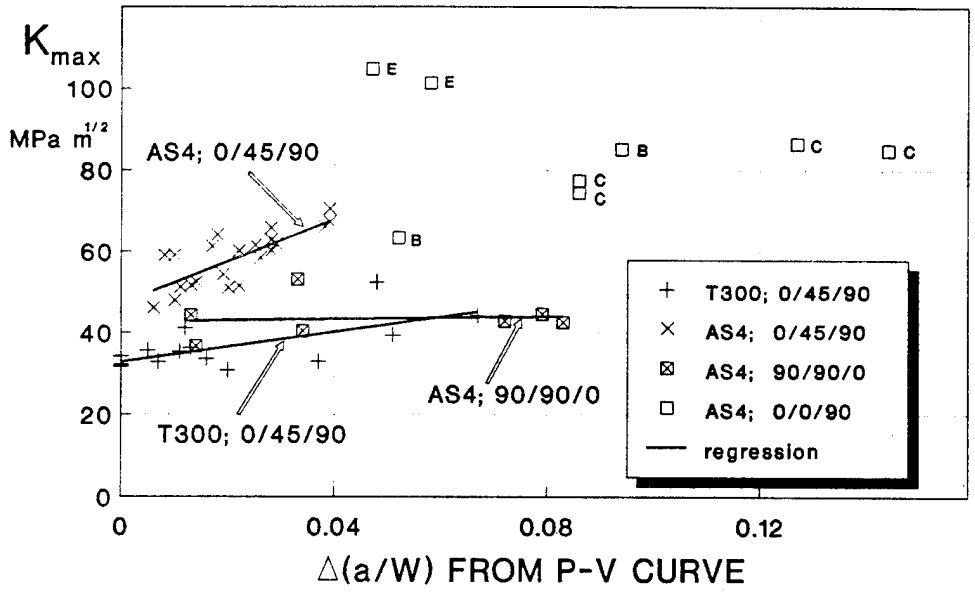

FIG. 13 - *Correspondence of applied K and calculated crack growth at point of maximum load*

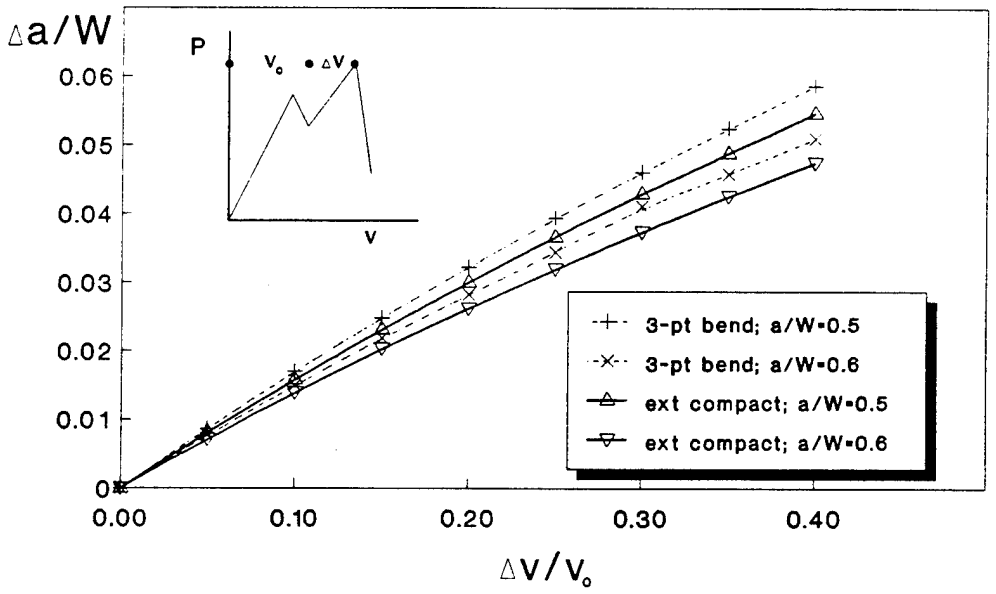

FIG. 14 - *Calculated crack growth corresponding to relative change in crack-mouth-opening displacement*

TECHNICAL REPORT INTERNAL DISTRIBUTION LIST

	NO. OF COPIES
CHIEF, DEVELOPMENT ENGINEERING DIVISION	
ATTN: AMSTA-AR-CCB-DA	1
-DB	1
-DC	1
-DD	1
-DE	1
CHIEF, ENGINEERING DIVISION	
ATTN: AMSTA-AR-CCB-E	1
-EA	1
-EB	1
-EC	
CHIEF, TECHNOLOGY DIVISION	
ATTN: AMSTA-AR-CCB-T	2
-TA	1
-TB	1
-TC	1
TECHNICAL LIBRARY	
ATTN: AMSTA-AR-CCB-O	5
TECHNICAL PUBLICATIONS & EDITING SECTION	
ATTN: AMSTA-AR-CCB-O	3
OPERATIONS DIRECTORATE	
ATTN: SMCWV-ODP-P	1
DIRECTOR, PROCUREMENT & CONTRACTING DIRECTORATE	
ATTN: SMCWV-PP	1
DIRECTOR, PRODUCT ASSURANCE & TEST DIRECTORATE	
ATTN: SMCWV-QA	1

NOTE: PLEASE NOTIFY DIRECTOR, BENÉT LABORATORIES, ATTN: AMSTA-AR-CCB-O OF ADDRESS CHANGES.

TECHNICAL REPORT EXTERNAL DISTRIBUTION LIST

	NO. OF COPIES
ASST SEC OF THE ARMY RESEARCH AND DEVELOPMENT ATTN: DEPT FOR SCI AND TECH THE PENTAGON WASHINGTON, D.C. 20310-0103	1
ADMINISTRATOR DEFENSE TECHNICAL INFO CENTER ATTN: DTIC-OCP (ACQUISITION GROUP) BLDG. 5, CAMERON STATION ALEXANDRIA, VA 22304-6145	2
COMMANDER U.S. ARMY ARDEC ATTN: SMCAR-AEE	1
SMCAR-AES, BLDG. 321	1
SMCAR-AET-O, BLDG. 351N	1
SMCAR-FSA	1
SMCAR-FSM-E	1
SMCAR-FSS-D, BLDG. 94	1
SMCAR-IMI-I, (STINFO) BLDG. 59 PICATINNY ARSENAL, NJ 07806-5000	2
DIRECTOR U.S. ARMY RESEARCH LABORATORY ATTN: AMSRL-DD-T, BLDG. 305 ABERDEEN PROVING GROUND, MD 21005-5066	1
DIRECTOR U.S. ARMY RESEARCH LABORATORY ATTN: AMSRL-WT-PD (DR. B. BURNS) ABERDEEN PROVING GROUND, MD 21005-5066	1
DIRECTOR U.S. MATERIEL SYSTEMS ANALYSIS ACTV ATTN: AMXSY-MP ABERDEEN PROVING GROUND, MD 21005-5071	1
COMMANDER ROCK ISLAND ARSENAL ATTN: SMCRI-ENM ROCK ISLAND, IL 61299-5000	1
MIAC/CINDAS PURDUE UNIVERSITY P.O. BOX 2634 WEST LAFAYETTE, IN 47906	1
COMMANDER U.S. ARMY TANK-AUTMV R&D COMMAND ATTN: AMSTA-DDL (TECH LIBRARY) WARREN, MI 48397-5000	1
COMMANDER U.S. MILITARY ACADEMY ATTN: DEPARTMENT OF MECHANICS WEST POINT, NY 10966-1792	1
U.S. ARMY MISSILE COMMAND REDSTONE SCIENTIFIC INFO CENTER ATTN: DOCUMENTS SECTION, BLDG. 4484 REDSTONE ARSENAL, AL 35898-5241	2
COMMANDER U.S. ARMY FOREIGN SCI & TECH CENTER ATTN: DRXST-SD 220 7TH STREET, N.E. CHARLOTTESVILLE, VA 22901	1
COMMANDER U.S. ARMY LABCOM MATERIALS TECHNOLOGY LABORATORY ATTN: SLCMT-IML (TECH LIBRARY) WATERTOWN, MA 02172-0001	2
COMMANDER U.S. ARMY LABCOM, ISA ATTN: SLCIS-IM-TL 2800 POWER MILL ROAD ADELPHI, MD 20783-1145	1

NOTE: PLEASE NOTIFY COMMANDER, ARMAMENT RESEARCH, DEVELOPMENT, AND ENGINEERING CENTER, BENÉT LABORATORIES, CCAC, U.S. ARMY TANK-AUTOMOTIVE AND ARMAMENTS COMMAND, AMSTA-AR-CCB-O, WATERVLIET, NY 12189-4050 OF ADDRESS CHANGES.

TECHNICAL REPORT EXTERNAL DISTRIBUTION LIST (CONT'D)

	NO. OF COPIES
COMMANDER U.S. ARMY RESEARCH OFFICE ATTN: CHIEF, IPO P.O. BOX 12211 RESEARCH TRIANGLE PARK, NC 27709-2211	1
DIRECTOR U.S. NAVAL RESEARCH LABORATORY ATTN: MATERIALS SCI & TECH DIV CODE 26-27 (DOC LIBRARY) WASHINGTON, D.C. 20375	1 1
WRIGHT LABORATORY ARMAMENT DIRECTORATE ATTN: WL/MNM EGLIN AFB, FL 32542-6810	1
WRIGHT LABORATORY ARMAMENT DIRECTORATE ATTN: WL/MNMF EGLIN AFB, FL 32542-6810	1

NOTE: PLEASE NOTIFY COMMANDER, ARMAMENT RESEARCH, DEVELOPMENT, AND ENGINEERING CENTER, BENÉT LABORATORIES, CCAC, U.S. ARMY TANK-AUTOMOTIVE AND ARMAMENTS COMMAND, AMSTA-AR-CCB-O, WATERVLIET, NY 12189-4050 OF ADDRESS CHANGES.